

Visualization of flow during cleaning process on a liquid nanofibrous filter

P Bílek

Department of Nanotechnology and Informatics, Institute for Nanomaterials,
Advanced Technology and Innovation, Technical University of Liberec, Studentská
1402/2, 461 17, Liberec, Czech Republic

petr.bilek@tul.cz

Abstract. This paper deals with visualization of flow during cleaning process on a nanofibrous filter. Cleaning of a filter is very important part of the filtration process which extends lifetime of the filter and improve filtration properties. Cleaning is carried out on flat-sheet filters, where particles are deposited on the filter surface and form a filtration cake. The cleaning process dislodges the deposited filtration cake, which is loose from the membrane surface to the retentate flow. The blocked pores in the filter are opened again and hydrodynamic properties are restored. The presented optical method enables to see flow behaviour in a thin laser sheet on the inlet side of a tested filter during the cleaning process. The local concentration of solid particles is possible to estimate and achieve new information about the cleaning process. In the article is described the cleaning process on nanofibrous membranes for waste water treatment. The hydrodynamic data were compared to the images of the cleaning process.

1. Introduction

Cleaning of a filter is very important part of the filtration process which extends lifetime of the filter and improve filtration properties. Cleaning is generally performed on flat-sheet filters, where particles are deposited on the filter surface and form a filtration cake. The cleaning process dislodges the deposited filtration cake, which is loose from the membrane surface to retentate flow. The blocked pores in the filter are opened again and hydrodynamic properties are restored. On the other hand the bulk filters are usually disposable, particles inside cannot be sufficiently removed. In the articles [1, 6] is described a back flow method for cleaning of air filters. The cleaning method is applied when either at a pressure drop limit or after a time interval. The filter surface is treated by laminating, calendaring, coating or singeing to improve filtration properties as mechanical robustness and filtration cake removal. The filter cleaning efficiency was determined according to residual pressure drop [6].

Direct visual observation (DVO) was used for investigation of back-pulse cleaning method [2]. DVO is useful tool for better understanding of the processes on the filter. The optimization of cleaning process was carried out by changing back pulse duration, pressure drop and shear velocity rates. It was found that multiple short back-pulses were more effective than fewer longer back-pulses at high cross-flow rate. However if the cross-flow rate is low it applies vice versa. The goal was to find an optimal duration between back-flow and permeate flow in order to total net flow of a filter be as high as



possible. Forward filtration flux versus membrane surface covered by filtration cake determined by DVO had linear form in [3].

Back-pulsation as a cleaning method was also used in [4, 5]. Chromium hydroxide particles were separated by a ceramic membrane in a cross-flow channel and the cleaning was carried out by a periodical back-pulsing in [4]. It was also found out that the larger pore diameter is used, the higher efficiency the back-pulsing is at high shear velocities 6.5 m/s. The time of the cleaning decreases with an increase back-pulse pressure and membrane pore diameter. Cleaning interval is strongly dependant on intensity of back-pulse, pore diameter and permeate flow for waste water. Milk was filtered by a reversed asymmetric membrane in [5]. The advantage is in lower cake resistance, which is formed inside the support layer. Optimization of the cleaning process during a solid-liquid separation was carried out in [7].

In this article the visualization of the cleaning process is performed by a laser sheet and a digital camera. This optical method enables to see flow behavior in a thin laser sheet on inlet side of a tested filter during the cleaning process. This optical method brings overall view and new information about cleaning processes on filters. More about the visualization of flow and laser anemometry is written in [8, 9]. Experiments are performed on a pilot setup for waste water treatment.

2. Experimental setup

The scheme of the filtration setup is shown in figure 1. Contaminated water is stored in a tank and the circuit 1 serves for cooling of a submerged pump and for treating water by a germicidal unit (UVC, 18 W). The circuit 2 is the main filtration circuit.

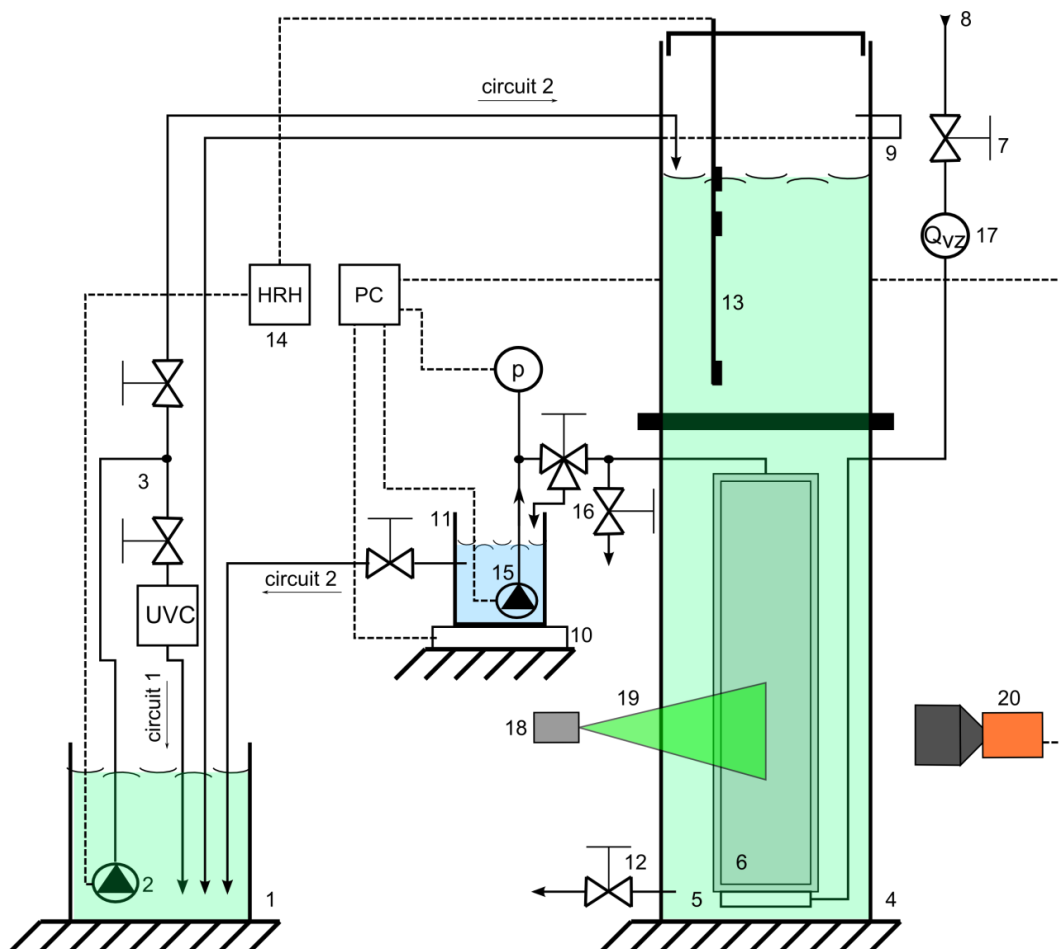


Figure 1. Scheme of the water filtration setup with the visualization system.

The sample of a tested filter is mounted into the filtration chamber. Numbers in figure 1 are explained subsequently - 1: Reserve tank for contaminated water, 2: Submerged pump 240 V, 3: Manual ball valves for raw set of flow in the circuit 1 and 2, 4: Filtration chamber, 5: Perforated tube serves as an air bubble maker, 6: A nanofibrous filter mounted on a plastic frame, 7: pressure reducer, 8: Compressed air supply, 9: Safety valve, 10: digital scale, 11: Measuring cylinder, 12: Outlet valve, 13: Probe for a water level indicator, 14: Water level indicator, 15: Submerged pump for backflow, 16: Ball valves, 17: Digital air flowmeter Testo 6441, 18: Laser module, 19: Laser sheet, 20: Digital camera.

Pressure drop is set by a height of the water level. The water level is controlled by unit HRH-1 and is more-less constant (500 mm), so the pressure drop Δp [kPa] is also constant (5 kPa). During the tests the flow Q_v [m^3/s] through the tested membrane is measured by a digital scale PCB 10000-1. Concentration of particles in inlet C_1 [ug/l] and outlet C_2 is measured by a laboratory nephelometer. Cleaning of the filter is performed by air bubbles and by reverse flow, which is set by a small submerged pump for 12 V. Inverse pressure drop on the filter is measured by a sensor GMSD 350 MRE, Greisinger. Ball valve serves for taking away samples of water for analysis. Compressed air is brought into the filter chamber and leads to a perforated tube under the filter frame. Air bubbles avoid growing of a dense filtration cake on the inlet side of the tested filter. Air flow is stopped only during the visualization process because of better visibility.

The cleaning process is investigated in the filter chamber, where an optical access is allowed, seen in figure 2. The flow in the vicinity of the tested filter is illuminated by the laser sheet generated by a 30° wobble angle Powell lens and a LED laser module (532 nm, 121 mW). The illuminated area is recorded by the digital camera (Pike F-210B/C, 50 fps, 1920 × 1080 px) equipped by lens (Samyang 35 mm, F1.4).



Figure 2. Picture of the filtration chamber from plexiglass and the visualization system.

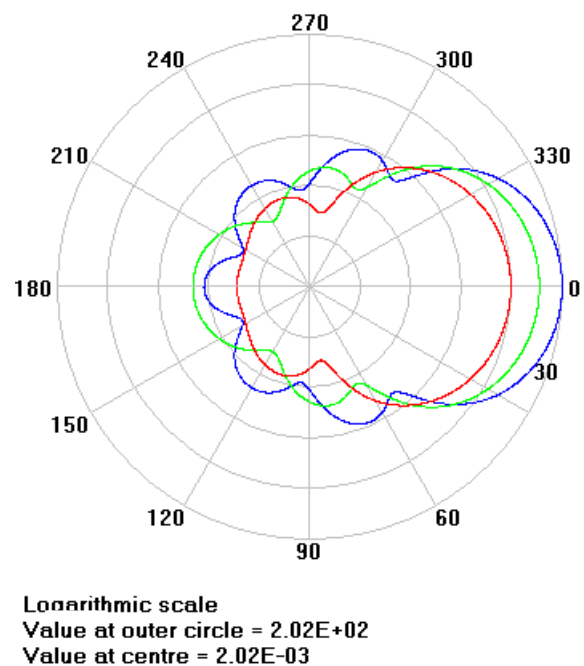


Figure 3. Scattering diagrams for polystyrene particles (green line - 0.5 μm , blue line - 0.6 μm and red line - 0.4 μm), generated by MiePlot software [11].

3. Experimental and results

3.1. Materials and methods

The tested filter is composed from two layers: an active nanofibrous and a support microfibrinous layer. Nanofibrous filter is made of polyamide and the support layer is made of polypropylene. The nanofibrous layer, made by electrospinning technique, was pressed on the support layer and it was laminated. Mean pore size is $0.4 \mu\text{m}$ and the maximum pore size is $0.8 \mu\text{m}$. Air permeability is $6.5 - 8 \text{ m/s} \cdot \text{Pa}$. An active area of the one filter module was 0.2 m^2 (two filter samples $10 \times 100 \text{ cm}$ mounted on a frame from the each side).

The testing water was composed from distilled water and artificial particles. The monodisperse polystyrene particles are easier detected by a nephelometer compared to the bacteria in real waste water. The analysis of this model water is faster and cheaper. According to the Mie theory the $0.5 \mu\text{m}$ particles are the most suitable [10]. They scatter sufficient amount of light in a laser sheet as well as they are small enough to simulate most of bacteria in water. The scattering diagram is seen in figure 3.

The duration of the experiment was 3 days. Flow rate and filtration efficiency were measured. The inlet side of the filter was cleaned by air bubbles and flow-rate of air was 50 litres per minute. In addition the filter module was three times cleaned by reverse flow after 2, 20 and 50 hours. Reverse pressure drop during the reverse flow was 7 kPa and lasts 3 minutes. More over the inlet side of the filter was visualized during backflow.

3.2. Flowrate and filtration efficiency

Flowrate was measured by digital scales. Filtration efficiency was calculated from mass concentration measured by a nephelometer. The filtration efficiency was measured mainly for the confidence, that the filtration samples are not damaged during the tests and the value of flowrate is not changed and distorted. The filtration efficiency was 98 %.

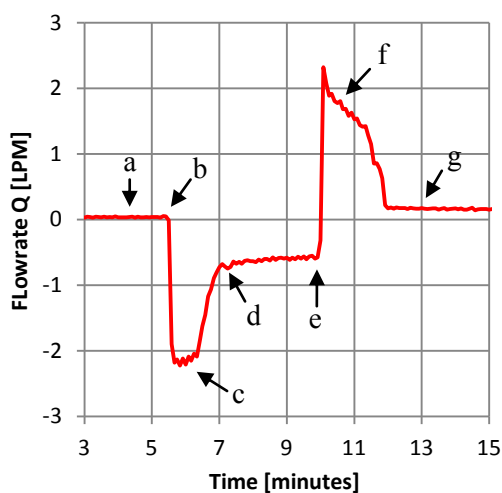


Figure 4. Graph of flowrate versus time during the cleaning process by reverse flow.

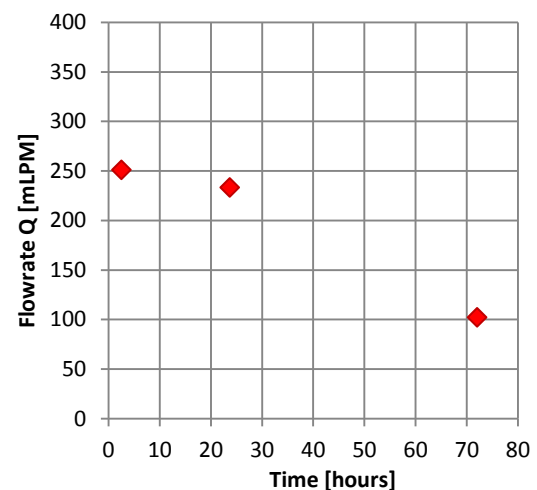


Figure 5. Points of flowrate (2, 20 and 50 hours) versus time after the cleaning of a filter.

A graph of flowrate during the cleaning process is seen on figure 4. Flowrate of blocked membrane is very low 20 mLPM (a). At point (b) inverse pressure drop was activated. The high inverse flowrate (c) is caused by an elasticity of the membrane. The membrane module is gradually filled by water. At point (d) the membrane module is full of water and the reverse flow passes only through the membrane. The cleaning process starts at this point. Reverse pressure drop is deactivated (e). High

flowrate is caused by draining of the membrane module (f). The regenerated flowrate of the cleaned membrane is seen at point (g). The reverse flow is started at point (b), but the cleaning process begins at point (d), almost one minute after the starting of reverse flow. The cleaning process lasts three minutes and ends at point (e), where reverse pressure drop is deactivated. We can see the inertia of flow in the membrane module, which is caused by elastic filters. The inertia of flow caused losses of the total permeability of the filtration module. The filtration module has to accept a lot of water before the cleaning process is activated. It extends a necessary time for the cleaning. Flowrate of the regenerated membrane (10 minutes after the cleaning process) in time is seen on figure 5.

3.3. Visualization of the cleaning process

Visualization of the inlet side of a filter during reverse flow (20 hours after the last cleaning by reverse flow) is seen on figure 6. We can see four images of the inlet side of the filter and each image is taken after 20 seconds. The filtration cake is gradually dislodged from the filter surface. We can see in the first image, that the filtration cake is still deposited on the surface. In 20 seconds later (second image) the filtration cake is partially released and it divaricates from the surface on next two images. The most important part of the cleaning process by reverse flow is at the beginning.

We can see three images (figure 7) of the cleaning process, where the reverse flow was applied after 2, 20 and 50 hours. It is seen not so much significant change of amount of dislodging particles in first two images (2 h and 20 h). The significant change is seen on the third picture (50 h). The decline of amount of dislodged particles is caused by a dense filtration cake, which was remained on the filter after cleaning by reverse flow. The pictures correspond with flowrates values on figure 5, also the first two flowrates are almost the same, but the flowrate after 50 h is much lower because of the insufficient cleaning.

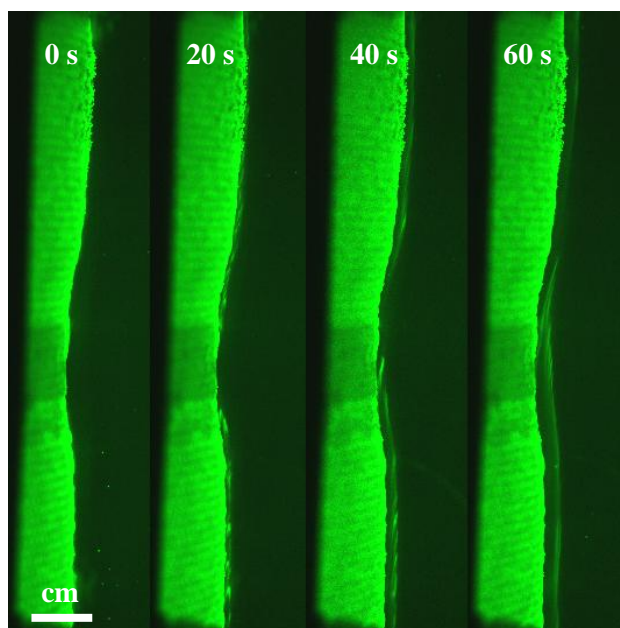


Figure 6. The first four pictures of the inlet side of a filter during cleaning by reverse flow.

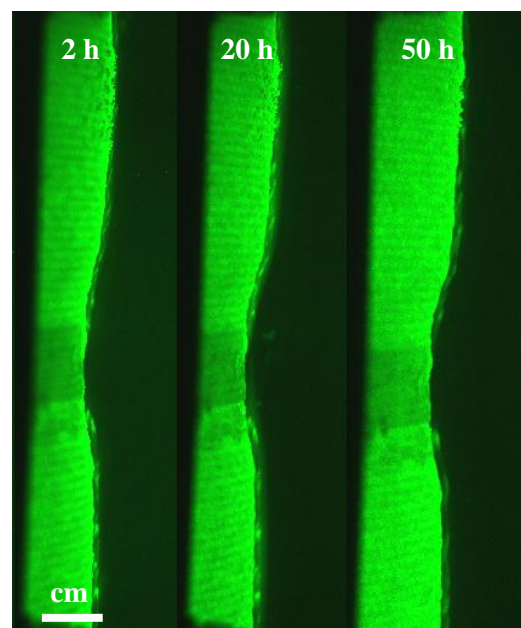


Figure 7. Three pictures of the inlet side of a filter after 2, 20 and 50 hours of filtering.

4. Conclusion

Cleaning of a filter is performed on flat-sheet filters, where particles are deposited on the inlet filter side, form a filtration cake, which blocks pores and significantly decreases permeability. The cleaning process keeps the filter surface clean and limits the growth of the filtration cake. In this article, the visualization was used to see the cleaning process in time for better description of the cleaning

process. The optical method is a promising tool for achievement new information about the cleaning mechanism. The method enables to visualize flow in the vicinity of the inlet side of a filter and measure the local concentration of testing particles. The visualization system described in the article is different compared to the direct observations methods in [2, 3]. Visualization is performed by a laser sheet and the digital camera. The experiments were carried out in a pilot filtration plant used to clean waste water.

The hydrodynamic data were compared to the images of the cleaning process during the experiment on a pilot setup for waste water treatment. Most of the particles are dislodged from filter surface at the beginning of the cleaning process and farther cleaning causes minimum dislodging of the particles. The result is similar as in [3]. The beginning of the cleaning process is the most important and it is not necessary to stress the membrane furthermore. The cleaning process is more effective when a filter is cleaned shortly and sufficiently often. It is seen that 50 h is to long time interval, which caused irreversible clogged filter.

Acknowledgments

The results of this project LO1201 were obtained through the financial support of the Ministry of Education, Youth and Sports in the framework of the targeted support of the “National Programme for Sustainability I”.

References

- [1] Hau C W-Y and Leung W W-F 2016 Experimental investigation of backpulse and backblow cleaning of nanofiber filter loaded with nano-aerosols *Separation and Purification Technology* vol **163** pp 30-38
- [2] Mores W D and Davis R H 2002 Yeast foulant removal by backpulses in crossflow microfiltration *Journal of Membrane Science* vol **208** Issues 1–2 pp 389-404
- [3] Mores W D and Davis R H 2001 Direct visual observation of yeast deposition and removal during microfiltration *Journal of Membrane Science* vol **189** Issue 2 pp 217-230
- [4] Sondhi R and Bhave R 2001 Role of backpulsing in fouling minimization in crossflow filtration with ceramic membranes *Journal of Membrane Science* vol **186** Issue 1 pp 41-52
- [5] Guerra A, Jonsson G, Rasmussen A, Nielsen E W and Edelsten D 1997 Low cross-flow velocity microfiltration of skim milk for removal of bacterial spores *International Dairy Journal* vol **7** Issue 12 pp 849-861
- [6] Cirqueira S S R, Tanabe E H and Aguiar M L 2017 Evaluation of operating conditions during the pulse jet cleaning filtration using different surface treated fibrous filters *Process Safety and Environmental Protection* vol **105** pp 69-78
- [7] Mores W D, Bowman C N and Davis R H 2000 Theoretical and experimental flux maximization by optimization of backpulsing *Journal of Membrane Science* vol **165** Issue 2 pp 225-236
- [8] Tropea C, Yarin A L and Foss J F 2007 Springer handbook of experimental fluid mechanics *Springer science and business media* p 1557 ISBN: 978-3-540-25141-5
- [9] Martin J E and García M H 2009 Combined PIV/PLIF measurements of a steady density current front *Experimental fluids* vol **45** pp 265-276
- [10] Hulst H G van de 1957 Light Scattering by Small Particles *Wiley New York* p 470 ISBN: 0-486-64228-3
- [11] Laven P MiePlot software [online: 30.1.2017] URL: <<http://www.philiplaven.com/mieplot.htm>>.